Stability of DNA Duplexes Containing GG, CC, AA, and TT Mismatches

Anna Tikhomirova, Irina V. Beletskaya, and Tigran V. Chalikian*

Department of Pharmaceutical Sciences, Leslie Dan Faculty of Pharmacy, University of Toronto, 144 College Street, Toronto, Ontario M5S 3M2, Canada

Received February 13, 2006; Revised Manuscript Received May 11, 2006

ABSTRACT: We employed salt-dependent differential scanning calorimetric measurements to characterize the stability of six oligomeric DNA duplexes (5′-GCCGGA**X**TGCCGG-3′/5′-CCGGCA**Y**TCCGGC-3′) that contain in the central **XY** position the GC, AT, GG, CC, AA, or TT base pair. The heat-induced helix-to-coil transitions of all the duplexes are associated with positive changes in heat capacity, ΔC_p, ranging from 0.43 to 0.53 kcal/mol. Positive values of ΔC_p result in strong temperature dependences of changes in enthalpy, $\Delta H°$, and entropy, $\Delta S°$, accompanying duplex melting and cause melting free energies, $\Delta G°$, to exhibit characteristically curved shapes. These observations suggest that ΔC_p needs to be carefully taken into account when the parameters of duplex stability are extrapolated to temperatures distant from the transition temperature, T_M. Comparison of the calorimetric and van't Hoff enthalpies revealed that none of the duplexes studied in this work exhibits two-state melting. Within the context of the central A**X**T/T**Y**A triplet, the thermal and thermodynamic stabilities of the duplexes in question change in the following order: GC > AT > GG > AA ≈ TT > CC. Our estimates revealed that the thermodynamic impact of the GG, AA, and TT mismatches is confined within the central triplet. In contrast, the thermodynamic impact of the CC mismatch propagates into the adjacent helix domains and may involve 7−9 bp. We discuss implications of our results for understanding the origins of initial recognition of mismatched DNA sites by enzymes of the DNA repair machinery.

Despite the spectacular advances of structural studies that have shed light on the biochemistry of DNA repair, the initial recognition of lesions and mismatches remains poorly understood and much debated (*1*−*4*). Structure-based hypotheses attempt to explain the recognition of damaged and mismatched sites on the basis of geometric differences between aberrant sites and standard DNA (*5*−*7*). However, crystallographic and NMR evidence suggests that mispaired duplexes are structurally very similar to canonical DNA (*8*−*12*). In addition, structural models fail to rationalize the fact that most DNA repair enzymes exhibit a remarkable ability to correctly recognize and repair lesions or mismatches of markedly different size, shape, and structure. For example, *Escherichia coli* MutS interacts with a wide range of mismatches and insertion−deletion loops (*13*). Thus, structural considerations alone have not yet provided a sufficient basis for understanding the range of mechanisms utilized in DNA damage and mismatch recognition. It has been hypothesized that the initial recognition of damaged or mismatched base pairs operates, in addition to structural criteria, through detection of more subtle characteristics of damaged and mismatched DNA (*14*, *15*). In one hypothesis, a mispaired DNA creates a domain of dynamic and thermodynamic instability that represents a recognition element for the repair system (*16*−*19*). In this and related models, repair proteins exploit thermodynamic differences between the damaged and canonical sites that are often structurally indistinguishable (*1*−*3*, *5*). These models, although not universally accepted (*20*), identify local destabilization of the duplex as the common determinant in the substrate DNA that initially attracts the repair enzyme to the mispaired site for primary binding.

To assess the validity of the thermodynamic models of DNA repair, one needs to systematically study correlations between the parameters of duplex destabilization by a particular mismatch or a lesion and the efficacy of its recognition and repair by DNA repair enzymes. The rigorous way of tackling this problem is to correlate the duplex stability parameters $\Delta G°$, $\Delta H°$, and $\Delta S°$ (changes in free energy, enthalpy, and entropy, respectively, accompanying helix-to-coil transitions) with the respective parameters describing the binding of a DNA repair enzyme to the mismatched DNA site (ΔG_b, ΔH_b, and ΔS_b). It is essential that the physical parameters be compared at a common temperature; the values of $\Delta G°$, $\Delta H°$, and $\Delta S°$ must be extrapolated to the experimental temperature of protein−DNA association. To this end, one needs to account for the temperature dependences of $\Delta H°$ and $\Delta S°$ as reflected in changes in heat capacity [$\Delta C_p = (\partial \Delta H°/\partial T)_p = T(\partial \Delta S°/\partial T)_p$]. Their correct evaluation and extrapolation to temperatures distant from the melting temperature, T_M, require knowledge of changes in heat capacity, ΔC_p, accompanying helix-to-coil transitions of duplexes under question. This consideration is important in view of a large body of experimental and theoretical evidence suggesting that helix-to-coil transitions of nucleic acids are accompanied by changes in heat capacity (*21*−*30*).

Differential scanning calorimetry (DSC) provides the most rigorous way to measure the energetics of heat-induced

* To whom correspondence should be addressed. Telephone: (416) 946-3715. Fax: (416) 978-8511. E-mail: chalikan@phm.utoronto.ca.

10.1021/bi060304j CCC: $33.50
Published on Web 08/09/2006

order−disorder transitions in macromolecular systems (*31*−*33*). However, a survey of the literature reveals that the majority but not all of the thermodynamic investigations of DNA mismatches have been performed using UV absorbance-monitored melting experiments coupled with the model-dependent van't Hoff approach (*34*−*36*). The van't Hoff formalism is based on the two-state approximation of order−disorder transitions and, consequently, may lead to significant errors should the transition involve intermediates (*37*). In this respect, it should be noted that many oligomeric duplexes, in particular, those containing non-Watson−Crick base pairs, do not exhibit two-state melting behavior (*38*). In addition, the van't Hoff approach is not well suited to evaluating changes in heat capacity, ΔC_p. These factors may summarily contribute to the fact that current nearest neighbor-based predictive algorithms are most effective near 50 °C and become less efficient at lower temperatures (*35*). This situation is unfortunate; as noted above, to correlate duplex destabilization with the efficacy of DNA repair, one needs to extrapolate the energetic parameters of duplex stability to the experimental temperature of association of a damaged DNA with enzyme(s) of DNA repair machinery (usually, 25 °C). Such extrapolations need to be carried out in a rigorous, model-independent way. These considerations lead to the necessity of performing systematic differential scanning calorimetric investigations on DNA duplexes containing noncanonical base pairs and accumulating respective calorimetric databases on the sequence-specific and damage/mismatch-specific duplex thermodynamics.

Our ultimate goal is to investigate all 12 possible DNA mismatches as a function of sequence context. As the initial stage of these investigations, we study here the energetics of helix-to-coil transitions of six 13-mer DNA duplexes (5′-GCCGGA**X**TGCCGG-3′/5′-CCGGCA**Y**TCCGGC-3′) which contain in the central **XY** position the GC or AT canonical base pair or the GG, CC, AA, or TT homomismatch. Our choice of the specific parent sequence is based on the criteria of adequate thermal stability and low probability of formation of alternative duplex structures (hairpins, parallel structures, slipped duplexes, etc.). The central **XY** position is flanked by AT base pairs to maximize the destabilizing effect of the mismatches under question. We employ high-precision salt-dependent DSC measurements to characterize the thermodynamic profiles of helix-to-coil transitions ($\Delta G°$, $\Delta H°$, $\Delta S°$, and ΔC_p) of these duplexes as a function of temperature. We compare our results with similar data previously obtained from van't Hoff analyses of UV melting profiles. By relating the values of $\Delta G°$, $\Delta H°$, and $\Delta S°$ for the mismatched duplexes to those measured for their parent duplexes, we quantify duplex destabilization by a particular mismatch. We discuss implications of our results for the initial recognition of mismatched DNA sites by DNA repair enzymes.

EXPERIMENTAL PROCEDURES

Materials. All oligonucleotides were synthesized and cartridge purified by ACGT, Inc. (Toronto, ON). The purity of the DNA oligomers was additionally tested with native and denaturing 20% PAGE and native 3% agarose electrophoresis. The samples were stained with ethidium bromide. For all oligomers, the purity with respect to the presence of shorter or longer oligonucleotide strands was found to be higher than ~95−96% which corresponds to the upper limit of the sensitivity of electrophoretic techniques.

The concentrations of single-stranded oligonucleotides were determined spectrophotometrically using the extinction coefficients, ϵ_{260}, that had been calculated with an additive nearest neighbor procedure as described by R. Owczarzy (http://www.owczarzy.net/extinct.htm). When developing his additive procedure and deriving nearest neighbor coefficients, Owczarzy employed previously published experimental data (*39*−*43*). We used the following extinction coefficients, ϵ_{260}, for single-stranded oligonucleotides at 25 °C: 112 200 M^{-1} cm^{-1} for 5′-CCGGCATTCCGGC-3′, 122 900 M^{-1} cm^{-1} for 5′-GCCGGAATGCCGG-3′, 110 300 M^{-1} cm^{-1} for 5′-CCGGCACTCCGGC-3′, 121 600 M^{-1} cm^{-1} for 5′-GCCGGAGTGCCGG-3′, 117 100 M^{-1} cm^{-1} for 5′-GCCGGACTGCCGG-3′, 119 000 M^{-1} cm^{-1} for 5′-GCCGGATTGCCGG-3′, 116 100 M^{-1} cm^{-1} for 5′-CCGGCAATCCGGC-3′, and 114 800 M^{-1} cm^{-1} for 5′-CCGGCAGTCCGGC-3′.

Equimolar amounts of complementary single-stranded oligonucleotides were combined in buffer to obtain each individual duplex. Specifically, the following double-stranded oligonucleotides were prepared and studied: 5′-GCCGGA**G**TGCCGG-3′/5′-CCGGCA**C**TCCGGC-3′ (GC), 5′-GCCGGA**A**TGCCGG-3′/5′-CCGGCA**T**TCCGGC-3′ (AT), 5′-GCCGGA**G**TGCCGG-3′/5′-CCGGCA**G**TCCGGC-3′ (GG), 5′-GCCGGA**C**TGCCGG-3′/5′-CCGGCA**C**TCCGGC-3′ (CC), 5′-GCCGGA**A**TGCCGG-3′/5′-CCGGCA**A**TCCGGC-3′ (AA), and 5′-GCCGGA**T**TGCCGG-3′/5′-CCGGCA**T**TCCGGC-3′ (TT). The stoichiometry of duplex formation was verified by Job plots in 500 mM NaCl at 25 °C (not shown). These plots were constructed by mixing complementary single strands in a spectrophotometric cuvette and recording the resulting changes in UV absorption at 260 nm. The Job plots yielded a 1:1 stoichiometry for all double-stranded DNA complexes studied in this work.

Duplex solutions were exhaustively dialyzed against the buffer under study using Spectrapor dialysis tubing with a 1000 Da molecular mass cutoff (VWR Canada). The concentration of each double-stranded oligonucleotide was measured spectrophotometrically before the calorimetric experiment according to the following procedure. The duplex was heat-denatured in the spectrophotometer with the melting profile being monitored by UV absorption at 260 nm. The postdenaturational baseline was linearly extrapolated to 25 °C with the concentration of the duplex being evaluated by dividing the extrapolated value of absorption by the sum of the extinction coefficients of the two complementary strands.

Optical Spectroscopy. Optical absorbance and circular dichroism spectra were recorded using an Aviv model 14 DS spectrophotometer and model 62 DS spectropolarimeter, respectively (Aviv Associates, Lakewood, NJ). A 10 mm path length cell was used for all UV absorbance measurements. A cell with a path length of 1 mm was used for the CD measurements. For CD spectroscopic experiments, the oligonucleotide concentrations were on the order of ~50 μM.

Differential Scanning Calorimetry. Calorimetric melting experiments with the duplexes were performed at a scan rate of 1 °C/min using a Calorimetry Sciences Corp. (Provo, UT) model 6100 NanoDSCII differential scanning calorimeter with a nominal cell volume of 0.3 mL. All measurements were performed in a 10 mM cacodylic acid/sodium cacodylate buffer adjusted to pH 6.7 and containing 1 mM Na_2-

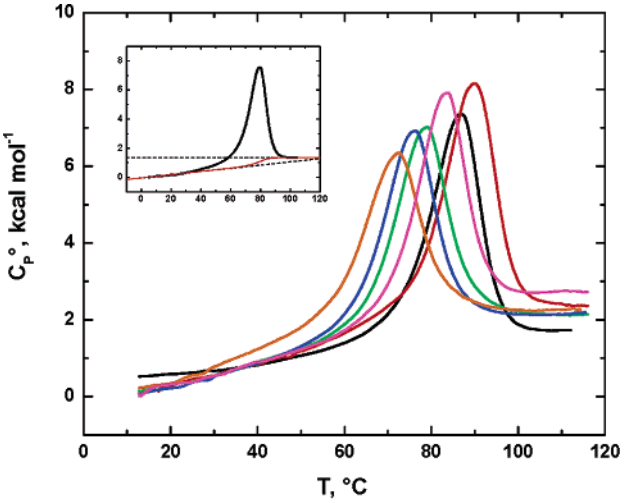

FIGURE 1: Representative differential scanning calorimetric melting profiles of the GC (red), AT (black), GG (magenta), CC (orange), AA (blue), and TT (green) duplexes at 1 M Na^+. The inset shows the DSC melting profiles of the AT duplex with outlined pre- and postdenaturational baselines.

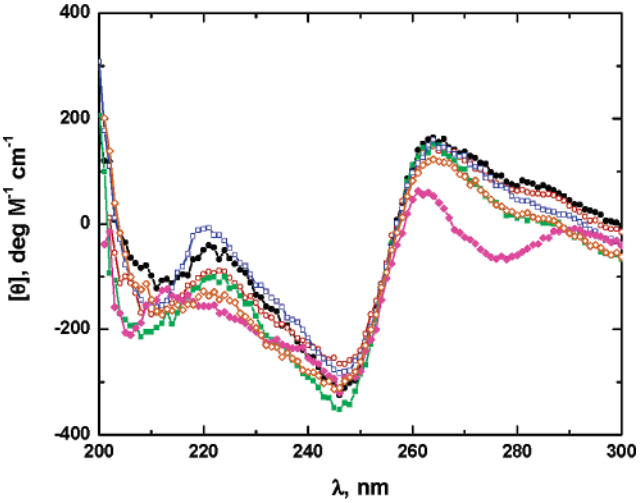

FIGURE 2: Circular dichroism spectra of the GC (red), AT (black), GG (magenta), CC (orange), AA (blue), and TT (green) duplexes at 1 M Na^+ and 25 °C.

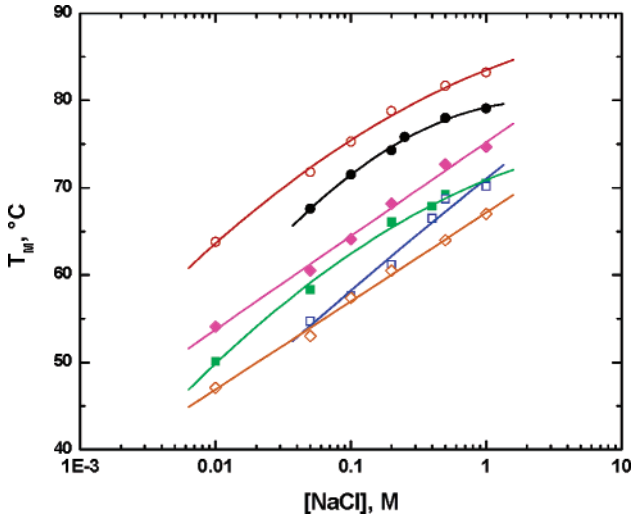

FIGURE 3: Dependences of melting temperatures of the GC (red), AT (black), GG (magenta), CC (orange), AA (blue), and TT (green) duplexes on sodium concentration.

EDTA and 10, 50, 100, 200, 500, or 1000 mM NaCl. DNA concentrations were on the order of 250 μM (~2 mg/mL). Appropriate buffer versus buffer baselines were determined prior to and immediately after the oligomer versus buffer scan and averaged. After subtraction of the buffer scan, the oligomer scan was normalized for concentration and analyzed as follows. A change in heat capacity, ΔC_p, was determined from the difference in the pre- and post-transition baselines both extrapolated to the midpoint of the transition (see the inset of Figure 1). The predenaturational baseline was drawn as a straight line outlined by the initial linear portion of the melting profile at the lowest possible temperature range. At higher temperatures, the shape of predenaturational baselines may deviate from linearity due to the heat-induced, noncooperative fraying of terminal base pairs. For all duplexes studied in this work, the postdenaturational baselines were essentially flat. Therefore, the postdenaturational baselines were drawn as horizontal lines coinciding with the single-stranded portions of the melting profiles. Figure 1 illustrates representative DSC thermograms recorded for the six oligomeric duplexes studied in this work at 1 M Na^+. The calorimetric enthalpy, ΔH_{cal}, was determined by integration of the area enclosed by the transition curve and the pre- and post-transition baselines, and the melting temperature, T_M, was determined as the temperature corresponding to the maximal heat capacity (*31*−*33*, *44*).

RESULTS

The CD spectra of the oligonucleotides at 1 M Na^+ are shown in Figure 2. Despite some differences that exist among the duplexes, the spectra suggest that the six duplexes are primarily in the B-form. Slight spectral differences between the duplexes are not unexpected given the fact that the CD spectrum of a duplex is a function of its nucleotide composition, sequence, and conformation (*45*, *46*). The absence of significant conformational differences between the mismatched and canonical duplexes is in agreement with previous reports (*12*). We thus conclude that the thermodynamic differences between the canonical and mismatched duplexes (see below) are not paralleled by equivalent alterations of structure.

Figure 3 shows the salt dependences of the calorimetrically determined melting temperature, T_M, for the six duplexes studied in this work. The values of T_M increase as the solution ionic strength increases. Interestingly, for the mismatched GG, AA, and CC duplexes, T_M changes linearly with log[Na^+], while the canonical GC and AT duplexes and the mismatched TT duplex exhibit nonlinear salt dependences. To the best of our knowledge, mismatched duplexes have not been investigated with respect to salt dependences of T_M in any systematic way. Therefore, it is difficult to judge the nature of the linear T_M versus log[Na^+] dependences of the GG, AA, and CC duplexes. For the moment, we take notice of this observation as a basis for future discussions.

Our measured nonlinear T_M versus log[Na^+] dependences for the AT and GC duplexes are in qualitative agreement with similar data reported by Owczarzy et al. (*47*) for a large number of canonical DNA duplexes. At 0.1 M Na^+, the average value of $\Delta T_M/\Delta$log[Na^+] for the oligonucleotides studied here is ~10.5. This number is within the range of

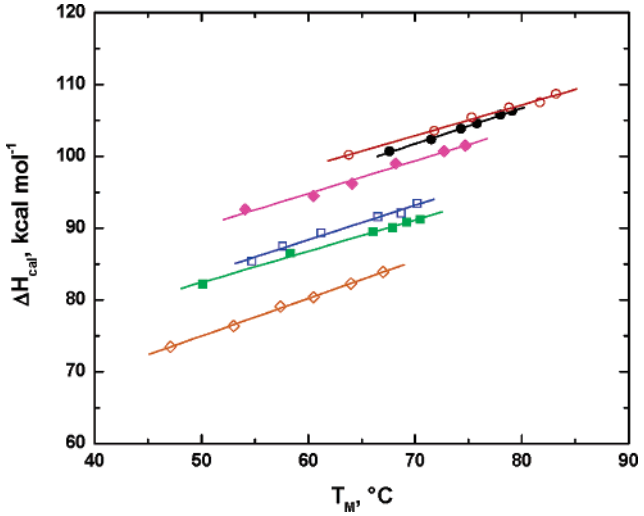

FIGURE 4: Dependences of the transition enthalpies of the GC (red), AT (black), GG (magenta), CC (orange), AA (blue), and TT (green) duplexes on melting temperature.

Table 1: Heat Capacity Changes Accompanying Helix-to-Coil Transitions of the Oligonucleotides Determined as the Slopes of the Temperature Dependences of Transition Enthalpies [ΔC_p(slope)] and as the Average Differences in the Pre- and Postdenaturation Baselines of the DSC Thermograms Recorded at Various Salt Concentrations [ΔC_p(DSC)]

DNA	ΔC_p(slope) (kcal mol^{-1} K^{-1})	ΔC_p(DSC) (kcal mol^{-1} K^{-1})
GC	0.43 ± 0.02	0.34 ± 0.05
AT	0.50 ± 0.02	0.54 ± 0.05
GG	0.45 ± 0.03	0.39 ± 0.09
CC	0.53 ± 0.01	0.32 ± 0.08
AA	0.48 ± 0.03	0.39 ± 0.09
TT	0.44 ± 0.02	0.40 ± 0.09

$\Delta T_M/\Delta\log[Na^+]$ values reported for short DNA duplexes (*47*) but significantly smaller than those observed for polymeric duplexes (between 16.7 and 21.2) (*22*).

Figure 4 plots transition enthalpies, $\Delta H°$, of the oligonucleotides against their melting temperatures, T_M. As is seen from Figure 4, the transition enthalpies exhibited by the canonical GC and AT duplexes are markedly higher than those exhibited by the four mismatch-containing duplexes. This observation is consistent with a picture in which a mismatch-containing duplex is enthalpically destabilized. For all duplexes, $\Delta H°$ changes linearly with T_M with the $\Delta H°/\Delta T_M$ slopes reflecting changes in heat capacity, ΔC_p, associated with the helix-to-coil transitions. Table 1 lists the values of ΔC_p determined as $\Delta H°/\Delta T_M$ as well as the average ΔC_p determined as the differences between the pre- and postdenaturational DSC baselines. The two modes of heat capacity determination yield comparable values.

DISCUSSION

Heat Capacity Changes. Inspection of data in Table 1 reveals that the average value of ΔC_p is 470 ± 35 cal mol^{-1} K^{-1} or 36 ± 3 cal (mol of base pairs)$^{-1}$ K^{-1}. Interestingly, the canonical AT and GC duplexes exhibit the lowest and highest values of ΔC_p, respectively, while the mismatched duplexes are characterized by intermediate values of ΔC_p. These observations may suggest the existence of a sequence-dependent component in ΔC_p. Currently, it is difficult to judge the significance of the observed sequence-dependent variation of ΔC_p. Further studies leading to the development of more extensive heat capacity databases on oligonucleotides will enable us to assess the relative importance of the sequence-dependent component in ΔC_p.

Table 2: Melting Temperatures (T_M) and Calorimetric (ΔH_{cal}) and van't Hoff (ΔH_{vH}) Enthalpies for a Family of DNA Duplexes with and without Mismatched Base Pairs at 1 M [Na^+]

DNA pair	T_M (°C)	ΔH_{cal} (kcal/mol)	ΔH_{vH} (kcal/mol)
GC	83.2 ± 0.4	108.7 ± 1.9	94.2 ± 2.0
AT	79.1 ± 0.4	106.3 ± 1.8	92.7 ± 1.7
GG	74.7 ± 0.4	101.5 ± 2.4	89.3 ± 2.3
CC	67.0 ± 0.4	83.9 ± 3.9	70.5 ± 4.1
AA	70.2 ± 0.4	93.4 ± 2.1	76.5 ± 2.2
TT	70.5 ± 0.4	91.2 ± 2.4	80.1 ± 1.5

The value of 36 ± 3 cal (mol of base pairs)$^{-1}$ K^{-1} is in qualitative but not quantitative agreement with 64 ± 8 cal (mol of base pairs)$^{-1}$ K^{-1}, the average ΔC_p for helix-to-coil transitions of polymeric nucleic acids (*21*, *22*). Despite its seemingly small magnitude, ΔC_p strongly affects the thermodynamic properties of helix-to-coil transitions of the duplexes. As discussed below, failure to account for ΔC_p leads to significant errors in determination of the transition enthalpy, entropy, and free energy, in particular, when these parameters are extrapolated to low and moderate temperatures.

Transition Temperatures. Inspection of Figure 3 reveals that, between 0.01 and 1 M Na^+, the GC duplex exhibits the highest thermal stability followed by the AT, GG, TT, AA, and CC duplexes. Between 0.05 and 1 M Na^+, the AA duplex is characterized by a T_M which is intermediate between those corresponding to the TT and CC duplexes. However, due to a steeper salt dependence of the T_M of the AA duplex, the T_M of the AA duplex exceeds that of the TT duplex at ≥1 M Na^+ and becomes smaller than that of the CC duplex at ≤0.05 M Na^+. At 1 M Na^+, the transition temperatures, T_M, for the GC, AT, GG, AA, TT, and CC duplexes are equal to 83.2 ± 0.2, 79.1 ± 0.2, 74.7 ± 0.2, 70.2 ± 0.2, 70.5 ± 0.2, and 67.0 ± 0.2 °C, respectively (see Table 2). This hierarchy is in qualitative agreement with previous reports on the relative thermal stabilities of the GG, CC, AA, and TT mismatches (*34*, *48*).

Nature of Helix-to-Coil Transitions of the Oligonucleotides. Comparison of the model-independent calorimetric, ΔH_{cal}, and model-dependent van't Hoff, ΔH_{vH}, enthalpies represents a robust way of examining the nature of a duplex melting process. If the process is two-state, the ratio of ΔH_{cal} to ΔH_{vH} is equal to unity (*49*). The $\Delta H_{cal}/\Delta H_{vH}$ ratio of >1 signifies the presence of intermediates between the pure double-stranded and pure single-stranded conformations and, consequently, deviation of the melting process from two-state. On the other hand, a $\Delta H_{cal}/\Delta H_{vH}$ of <1 is indicative of a process which involves aggregated double-stranded species.

We calculated the van't Hoff transition enthalpies from the shape of the calorimetric profiles using the relationship (*31*, *49*)

$$\Delta H_{vH} = (n^{1/2} + 1)T_M\{R[\langle C_p\rangle_{max} - \Delta C_p n^{1/2}/(n^{1/2} + 1)]\}^{1/2} \quad (1)$$

where n is the molecularity of the transition which, for duplex

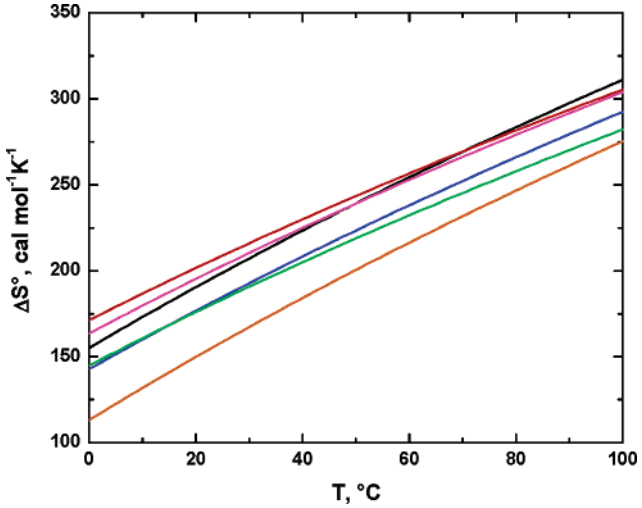

FIGURE 5: Temperature dependences of the transition entropies of the GC (red), AT (black), GG (magenta), CC (orange), AA (blue), and TT (green) duplexes.

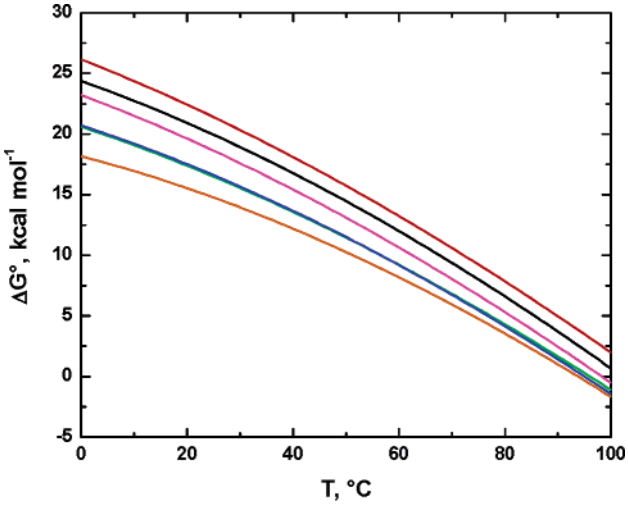

FIGURE 6: Temperature dependences of the transition free energies of the GC (red), AT (black), GG (magenta), CC (orange), AA (blue), and TT (green) duplexes.

melting, equals 2 and $\langle C_p \rangle_{max}$ is the maximal excess heat capacity at T_M.

Table 2 lists the melting temperatures, T_M, along with the calorimetric, ΔH_{cal}, and van't Hoff, ΔH_{vH}, transition enthalpies at 1 M Na^+. Inspection of data in Table 2 reveals that, for all duplexes, the calorimetric enthalpy, ΔH_{cal}, is higher than the van't Hoff enthalpy, ΔH_{vH}, with the $\Delta H_{cal}/\Delta H_{vH}$ ratio being within a range of 1.14−1.22. It should be noted that $\Delta H_{cal}/\Delta H_{vH}$ tends to increase with a decrease in salt concentration. For example, at 10 mM Na^+, the values of $\Delta H_{cal}/\Delta H_{vH}$ range from 1.20 to 1.40. The observed deviation of $\Delta H_{cal}/\Delta H_{vH}$ from unity suggests that, for the oligonucleotides studied in this work, the helix-to-coil transitions investigated in this work are not strictly two-state and involve intermediates. Consequently, the van't Hoff analysis of the stability characteristics of these duplexes may lead to errors in the determination of transition enthalpies, entropies, and free energies.

The observation that our duplexes do not display a two-state melting behavior is in agreement with results reported by the Breslauer and Privalov groups (*17*, *24*, *50*, *51*). Two-state melting is typically observed for canonical duplexes containing eight or fewer base pairs. For longer duplexes, the calorimetric and van't Hoff enthalpies may be significantly different (*50*). Duplexes containing lesions and adducts predominantly exhibit non-two-state melting transitions (*17*, *51*).

Changes in Enthalpy, Entropy, and Free Energy. Figures 5 and 6 present the temperature dependences of changes in entropy [$\Delta S° = \Delta H°/T_M + \Delta C_p \ln(T/T_M) + R \ln(C_T/4)$] and free energy {$\Delta G° = \Delta H°(1 - T/T_M) + \Delta C_p[T - T_M - T \ln(T/T_M)] - RT \ln(C_T/4)$} accompanying helix-to-coil transitions of the oligonucleotides at 1 M Na^+ ($\Delta H°$ is the calorimetric enthalpy; ΔC_p was determined as the $\Delta H°/\Delta T_M$ slopes in Figure 4).

Inspection of Figures 4−6 reveals that the values of $\Delta H°$, $\Delta S°$, and $\Delta G°$ are strongly temperature-dependent. The $\Delta G°$ versus T functions exhibit characteristically curved, parabolic-like shapes typical of the processes that are associated with positive changes in heat capacity, ΔC_p. Between 0 and 100 °C, GC is the most stable duplex (exhibits the highest $\Delta G°$ value) followed by the AT duplex and further by the GG, AA ≈ TT, and CC mismatched duplexes. This trend is in good agreement with previous reports (see ref *35*). Comparison of Figures 3 and 6 reveals that the $\Delta G°$-derived hierarchy of thermodynamic stabilities is in line with the relative order of thermal stabilities as outlined by T_M.

The observed thermal and/or thermodynamic stability hierarchy between the GG, AA, TT, and CC mismatches has been convincingly rationalized in structural terms (*34*). The purine GG and AA mismatches have higher stacking propensities relative to the pyrimidine TT and CC mismatches. On the other hand, the GG and TT mismatches are stabilized by two hydrogen bonds between the bases, while the AA and CC mismatches are stabilized by a single hydrogen bond (*34*). Consequently, the GG mismatch with a high stacking propensity and two hydrogen bonds exhibits the highest thermal and/or thermodynamic stability followed by the AA (high stacking potential with a single hydrogen bond) and TT (low stacking potential with two hydrogen bonds) mismatches. The CC mismatch with a low stacking potential and a single hydrogen bond exhibits the lowest stability.

Differential Stability of Canonical and Mismatched Duplexes. Figures 7−9 show the temperature dependences of the differential enthalpies, $\Delta\Delta H$, entropies, $\Delta\Delta S$, and free energies, $\Delta\Delta G$, of the mismatches and their respective Watson−Crick counterparts (GG−GC, CC−GC, AA−AT, and TT−AT). Table 3 compares two sets of data. The first set represents our differential mismatch versus parent duplex as well as GC versus AT values of $\Delta\Delta H$, $\Delta\Delta S$, and $\Delta\Delta G$ extrapolated to 37 °C. The second set of data was calculated at the same temperature using the nearest neighbor parameters presented by SantaLucia and co-workers (*34*, *35*). Inspection of data in Table 3 reveals a good agreement between our values and SantaLucia's values of $\Delta\Delta G$. However, there are discrepancies between the two sets of $\Delta\Delta H$ and $\Delta\Delta S$ values. These discrepancies probably reflect the $\Delta C_p = 0$ and two-state-ness assumptions about transitions used by SantaLucia and co-workers (*34*, *35*). Errors related to these assumptions appear to offset each other in $\Delta G°$, probably due to a phenomenon known as enthalpy−entropy compensation.

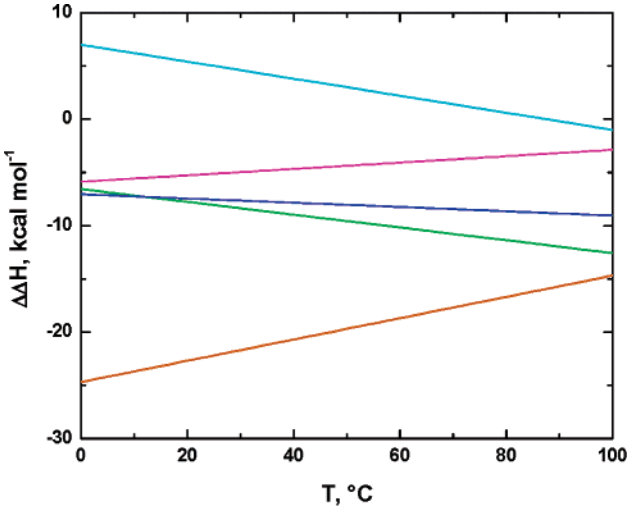

FIGURE 7: Temperature dependences of the differential transition enthalpies of the GG (magenta), CC (orange), AA (blue), and TT (green) duplexes and their appropriate parent duplexes.

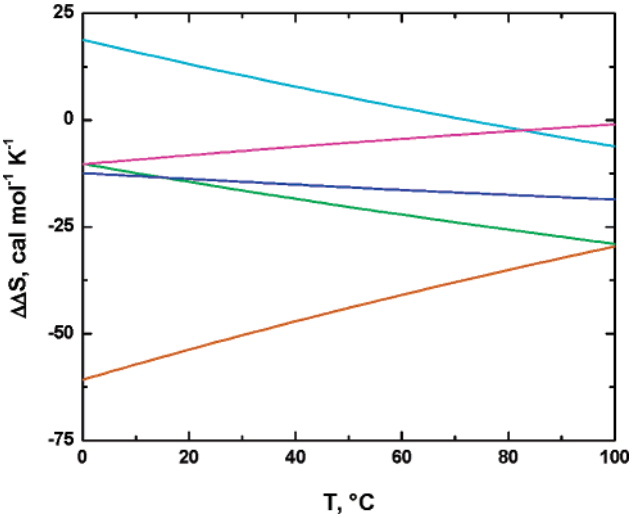

FIGURE 8: Temperature dependences of the differential transition entropies of the GG (magenta), CC (orange), AA (blue), and TT (green) duplexes and their appropriate parent duplexes.

Table 4 presents the differential mismatch versus parent duplex values of $\Delta\Delta H$, $\Delta\Delta S$, and $\Delta\Delta G$ at 25 °C, a commonly used experimental temperature. Inspection of thermodynamic data presented in Table 4 reveals that the differential transition free energy, $\Delta\Delta G$, of a mismatched duplex and its canonical counterpart is smaller in absolute magnitude than the respective differential transition enthalpy, $\Delta\Delta H$. For example, the differential values of $\Delta\Delta H$ and $\Delta\Delta G$ for the CC and GC duplexes are equal to −22.2 and −6.6 kcal/mol, respectively. This disparity, generally termed enthalpy−entropy compensation, suggests that the free energy penalty related to duplex destabilization is partly offset by a favorable entropic effect. The latter reflects a greater conformational flexibility (greater disorder) of mismatched sequences in their duplex state. It should be noted that enthalpy−entropy compensation is a common feature of helix-to-coil transitions of double-stranded nucleic acids, including duplexes containing mismatched or damaged base pairs (*18*, *38*).

The canonical GC duplex is 2.5−2.9 kcal/mol more stable than its mismatched counterpart GG duplex and 3.6−8.0 kcal/mol more stable than the CC duplex (see Figure 9). As seen in Figure 9, the differential GG versus GC $\Delta\Delta G$ value depends only slightly on temperature. In contrast, the CC versus GC value of $\Delta\Delta G$ exhibits a strong temperature dependence, increasing from −8.0 kcal/mol at 0 °C to −3.6 kcal/mol at 100 °C. Inspection of Figures 7 and 8 reveals that, for the GG and CC mismatches, the thermodynamic nature of destabilization is purely enthalpic. From the entropic point, the two mismatches are favored over their parent GC base pair. This observation is consistent with a picture in which the mismatched duplexes are characterized by a greater conformational entropy (flexibility) compared to the parent duplex. At 25 °C, the differential $\Delta\Delta G$ values for the GG and CC mismatches are −2.7 and −6.6 kcal/mol, respectively; the $\Delta\Delta H$ values are −4.9 and −22.2 kcal/

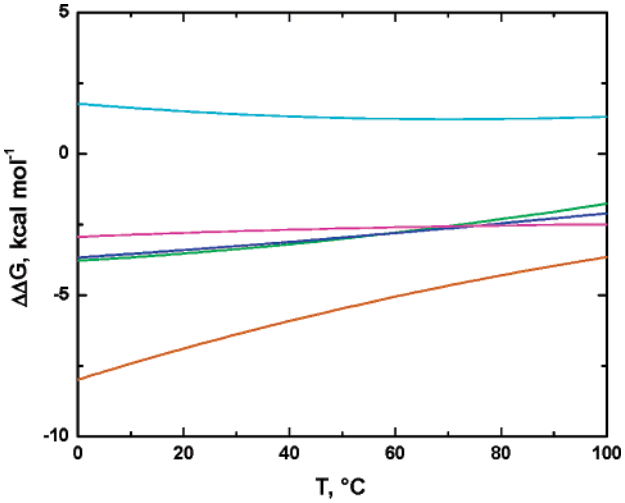

FIGURE 9: Temperature dependences of the differential transition free energies of the GG (magenta), CC (orange), AA (blue), and TT (green) duplexes and their appropriate parent duplexes.

Table 3: Comparison between the Differential Transition Enthalpies, Entropies, and Free Energies of Various Oligonucleotide Pairs at 37 °C from This Work and Calculated Using the Nearest Neighbor Approach

DNA pair	$\Delta\Delta H_{37}$ (kcal/mol)	$\Delta\Delta S_{37}$ (cal mol^{-1} K^{-1})	$\Delta\Delta G_{37}$ (kcal/mol)
GC·AT	4.0 ± 1.9[a]	8.7 ± 6.4[a]	1.3 ± 1.1[a]
	1.2[b]	1.5[b]	0.8[b]
GG·GC	−4.7 ± 2.4[a]	−6.5 ± 8.3[a]	−2.6 ± 1.2[a]
	−9.8[b]	−24.2[b]	−2.5[b]
CC·GC	−21.2 ± 3.9[a]	−48.0 ± 11.2[a]	−6.0 ± 1.5[a]
	−16.0[b]	−38.8[b]	−5.4[b]
AA·AT	−7.7 ± 2.1[a]	−14.9 ± 7.5[a]	−3.2 ± 1.2[a]
	−13.2[b]	−45.1[b]	−3.1[b]
TT·AT	−8.7 ± 2.4[a]	−17.9 ± 7.6[a]	−3.2 ± 1.2[a]
	−9.4[b]	−20.1[b]	−2.6[b]

[a] From this work. [b] Calculated using nearest neighbor parameters presented in ref *35*.

Table 4: Differential Transition Enthalpies, Entropies, and Free Energies of a Mismatch and Its Parent Duplex Extrapolated to 25 °C

DNA pair	$\Delta\Delta H_{25}$ (kcal/mol)	$\Delta\Delta S_{25}$ (cal mol^{-1} K^{-1})	$\Delta\Delta G_{25}$ (kcal/mol)
GG·GC	−5.1 ± 2.4	−7.7 ± 8.3	−2.8 ± 1.2
CC·GC	−22.2 ± 3.9	−52.0 ± 11.2	−6.6 ± 1.6
AA·AT	−7.5 ± 2.1	−14.1 ± 7.5	−3.3 ± 1.1
TT·AT	−8.1 ± 2.4	−15.5 ± 7.6	−3.5 ± 1.4

mol, respectively, while the $\Delta\Delta S$ values are −7.8 and −52.0 cal mol^{-1} K^{-1}, respectively.

Further inspection of Figure 9 reveals that the AA and TT duplexes exhibit very similar ΔG versus T dependences. The differential free energies, $\Delta\Delta G$, of the AA and TT duplexes and their parent AT duplex are both increasing functions of temperature. The values of $\Delta\Delta G$ for the AA and TT duplexes increase from −3.7 kcal/mol at 0 °C to ∼2.0 kcal/mol at 100 °C (see Figure 9). Comparison between Figures 7 and 8 reveals that, like that of GG and CC mismatches, destabilization of the AA and TT mismatches is purely enthalpic: $\Delta\Delta H$ (Figure 7) and $\Delta\Delta S$ (Figure 8) are both negative between 0 and 100 °C. At 25 °C, the differential $\Delta\Delta G$ values for the AA and TT mismatches are −3.3 and −3.5 kcal/mol, respectively; the $\Delta\Delta H$ values are −7.5 and −8.1 kcal/mol, respectively, while the $\Delta\Delta S$ values are −14.1 and −15.5 cal mol^{-1} K^{-1}, respectively.

Extent of Duplex Destabilization and Implications for DNA Repair. In this section, we compare the parameters of duplex destabilization by each of the mismatches with the stability characteristics of the two canonical duplexes. Such comparisons enable one to assess the extent of propagation of mismatch-induced duplex destabilization. Data graphically presented in Figures 3−6 enable one to evaluate the average stability parameters of the canonical AT and GC duplexes. At 25 °C, the average values of ΔH_{bp}, ΔS_{bp}, and ΔG_{bp} for these duplexes normalized per base pair are 6.3 ± 0.2 kcal/mol, 15.7 ± 0.4 cal mol^{-1} K^{-1}, and 1.6 ± 0.1 kcal/mol, respectively. If normalized per triplet, the values of ΔH_T ($3\Delta H_{bp}$), ΔS_T ($3\Delta S_{bp}$), and ΔG_T ($3\Delta G_{bp}$) become equal to 18.9 ± 0.6 kcal/mol, 47.1 ± 1.2 cal mol^{-1} K^{-1}, and 4.8 ± 0.3 kcal/mol, respectively.

At 25 °C, the values of $\Delta\Delta H$, $\Delta\Delta S$, and $\Delta\Delta G$ for the GG mismatch equal −5.1 kcal/mol, −7.7 cal mol^{-1} K^{-1}, and −2.8 kcal/mol, respectively (see Table 4). These values represent in absolute magnitude 26, 16, and 58% of ΔH_T, ΔS_T, and ΔG_T, respectively. For the AA mismatch, $\Delta\Delta H$, $\Delta\Delta S$, and $\Delta\Delta G$ are −7.5 kcal/mol, −14.1 cal mol^{-1} K^{-1}, and −3.3 kcal/mol, respectively, which, in absolute magnitude, represent 40, 30, and 69% of ΔH_T, ΔS_T, and ΔG_T, respectively. For the TT mismatch, $\Delta\Delta H$, $\Delta\Delta S$, and $\Delta\Delta G$ are −8.1 kcal/mol, −15.5 cal mol^{-1} K^{-1}, and −3.5 kcal/mol, respectively, which, in absolute magnitude, represent 43, 33, and 73% of ΔH_T, ΔS_T, and ΔG_T, respectively. Given the fact that $\Delta\Delta H$, $\Delta\Delta S$, and $\Delta\Delta G$ are significantly smaller in magnitude than ΔH_T, ΔS_T, and ΔG_T, we propose that thermodynamic destabilization of the GG, AA, and TT duplexes is effectively localized within the central A**X**G/T**Y**C triplet. With this notion, the average duplex destabilization per base pair within the central triplet (averaged over $\Delta\Delta H$, $\Delta\Delta S$, and $\Delta\Delta G$) is 43 ± 20% (∼45%).

In contrast to the GG, AA, and TT mismatches, the CC mismatch (the least stable mismatch) exhibits values of $\Delta\Delta H$, $\Delta\Delta S$, and $\Delta\Delta G$ which are substantially larger in magnitude than ΔH_T, ΔS_T, and ΔG_T, respectively. Specifically, for this mismatch, $\Delta\Delta H$, $\Delta\Delta S$, and $\Delta\Delta G$ are −22.2 kcal/mol, −52.0 cal mol^{-1} K^{-1}, and −6.6 kcal/mol, respectively, which, in absolute magnitude, represent 117, 110, and 137% of ΔH_T, ΔS_T, and ΔG_T, respectively. These disparities cannot be rationalized within the limits of the central A**X**G/T**Y**C triplet. In fact, the observed disparities are so large that they suggest that thermodynamic destabilization of the duplex by the CC mismatch is delocalized and propagates beyond the A**X**G/T**Y**C triplet. As a first approximation, one may assume that each affected base pair is destabilized by ∼45% (as in the case of GG, AA, and TT). With this approximation, the extent of propagation can be estimated by dividing the absolute values of $\Delta\Delta H$, $\Delta\Delta S$, and $\Delta\Delta G$ for the CC duplex (−22.2 kcal/mol, −52.0 cal mol^{-1} K^{-1}, and −6.6 kcal/mol, respectively) by ∼45% of ΔH_{bp}, ΔS_{bp}, and ΔG_{bp} (2.8 kcal/mol, 7.1 cal mol^{-1} K^{-1}, and 0.7 kcal/mol, respectively), respectively. This rough estimate suggests that the thermodynamic destabilization of the CC duplex involves 7−9 bp.

These estimates have implications for DNA repair and the mechanisms underlying the initial recognition of noncanonical sites by mismatch repair proteins, such as MutS. Within the framework of the thermodynamic hypothesis of DNA repair, a damaged or mismatched DNA site creates a domain of thermodynamic instability that represents a recognition element for the repair system (*4*, *16*−*19*). In this model, repair proteins are thought to exploit energetic differences between the mispaired and canonical sites that might be otherwise structurally indistinguishable. Our observation that some mismatches are localized while others are delocalized with respect to the extent of their thermodynamic impact may additionally challenge and put constraints on the ability of a repair protein to recognize and bind to a damaged DNA site. It should be noted that propagation of thermodynamic destabilization of a duplex by a mismatched or damaged base pair into the adjacent helix domains (as reflected in disproportionally large decreases in the transition enthalpy and free energy) has been reported for DNA duplexes containing GA mismatches, abasic lesions, and oxidatively damaged guanosine and exocyclic cytosine adducts (*17*, *38*, *51*).

CLOSING REMARKS

We used salt-dependent differential scanning calorimetric measurements to characterize destabilization of oligomeric DNA duplexes due to the presence of the GG, CC, AA, and TT homomismatches in the central position. The DNA systems that were studied include six 13-mer duplexes (5′-GCCGGA**X**TGCCGG-3′/5′-CCGGCA**Y**TCCGGC-3′) in which the central position **XY** is occupied by a GC, AT, GG, CC, AA, or TT base pair. Our calorimetric measurements revealed that all duplexes are characterized by nonzero changes in heat capacity, ΔC_p, ranging from 0.43 to 0.53 kcal/mol. Positive values of ΔC_p lead to strong temperature dependences exhibited by the $\Delta H°$ and $\Delta S°$ functions and characteristically curved shapes of the $\Delta G°$ functions. Comparison between the calorimetric and van't Hoff enthalpies revealed that the helix-to-coil transitions of both the canonical and the mismatched duplexes are not strictly two-state and involve intermediates.

Within the context of the central A**X**T/T**Y**A triplet, the thermal and thermodynamic stability of the duplexes studied in this work decrease in the following order: GC > AT > GG > AA ≈ TT > CC. All mismatches studied in this work are destabilized enthalpically. In contrast, the mismatches are entropically favored relative to their parent duplexes. Our estimates suggest that duplex destabilization by the GG, AA, and TT mismatches is predominantly confined within the central (A**X**G/T**Y**A) triplet. In contrast, duplex destabilization by the CC mismatch propagates into the adjacent helix

domains and may involve 7−9 bp. These results have implications for understanding the molecular origins of the initial recognition of mismatched base pairs by enzymes of the DNA repair machinery.

ACKNOWLEDGMENT

This investigation was supported by grants from CIHR and NSERC to T.V.C. I.V.B. acknowledges her postdoctoral support from the CIHR Protein Folding Training Program.

REFERENCES

1. Hsieh, P. (2001) Molecular mechanisms of DNA mismatch repair, *Mutat. Res. 486*, 71−87.
2. Schofield, M. J., and Hsieh, P. (2003) DNA mismatch repair: Molecular mechanisms and biological function, *Annu. Rev. Microbiol. 57*, 579−608.
3. Harfe, B. D., and Jinks-Robertson, S. (2000) DNA mismatch repair and genetic instability, *Annu. Rev. Genet. 34*, 359−399.
4. Rajski, S. R., Jackson, B. A., and Barton, J. K. (2000) DNA repair: Models for damage and mismatch recognition, *Mutat. Res. 447*, 49−72.
5. Buermeyer, A. B., Deschenes, S. M., Baker, S. M., and Liskay, R. M. (1999) Mammalian DNA mismatch repair, *Annu. Rev. Genet. 33*, 533−564.
6. Isaacs, R. J., and Spielmann, H. P. (2004) A model for initial DNA lesion recognition by NER and MMR based on local conformational flexibility, *DNA Repair 3*, 455−464.
7. Yang, W., Junop, M. S., Ban, C., Obmolova, G., and Hsieh, P. (2000) DNA mismatch repair: From structure to mechanism, *Cold Spring Harbor Symp. Quant. Biol. 65*, 225−232.
8. Skelly, J. V., Edwards, K. J., Jenkins, T. C., and Neidle, S. (1993) Crystal structure of an oligonucleotide duplex containing G•G base pairs: Influence of mispairing on DNA backbone conformation, *Proc. Natl. Acad. Sci. U.S.A. 90*, 804−808.
9. Prive, G. G., Heinemann, U., Chandrasegaran, S., Kan, L. S., Kopka, M. L., and Dickerson, R. E. (1987) Helix geometry, hydration, and GA mismatch in a B-DNA decamer, *Science 238*, 498−504.
10. Hunter, W. N., Brown, T., Anand, N. N., and Kennard, O. (1986) Structure of an adenine-cytosine base pair in DNA and its implications for mismatch repair, *Nature 320*, 552−555.
11. Brown, T., Kennard, O., Kneale, G., and Rabinovich, D. (1985) High-resolution structure of a DNA helix containing mismatched base pairs, *Nature 315*, 604−606.
12. Fazakerley, G. V., and Boulard, Y. (1995) DNA mismatches and modified bases, *Methods Enzymol. 261*, 145−163.
13. Lindahl, T. (1993) Instability and decay of the primary structure of DNA, *Nature 362*, 709−715.
14. Singer, B., and Hang, B. (1997) What structural features determine repair enzyme specificity and mechanism in chemically modified DNA? *Chem. Res. Toxicol. 10*, 713−732.
15. Mol, C. D., Parikh, S. S., Putnam, C. D., Lo, T. P., and Tainer, J. A. (1999) DNA repair mechanisms for the recognition and removal of damaged DNA bases, *Annu. Rev. Biophys. Biomol. Struct. 28*, 101−128.
16. Plum, G. E., and Breslauer, K. J. (1994) DNA lesions. A thermodynamic perspective, *Ann. N.Y. Acad. Sci. 726*, 45−55.
17. Plum, G. E., Grollman, A. P., Johnson, F., and Breslauer, K. J. (1995) Influence of the oxidatively damaged adduct 8-oxodeoxyguanosine on the conformation, energetics, and thermodynamic stability of a DNA duplex, *Biochemistry 34*, 16148−16160.
18. Pilch, D. S., Plum, G. E., and Breslauer, K. J. (1995) The thermodynamics of DNA structures that contain lesions or guanine tetrads, *Curr. Opin. Struct. Biol. 5*, 334−342.
19. Sagi, J., Hang, B., and Singer, B. (1999) Sequence-dependent repair of synthetic AP sites in 15-mer and 35-mer oligonucleotides: Role of thermodynamic stability imposed by neighbor bases, *Chem. Res. Toxicol. 12*, 917−923.
20. Kunkel, T. A., and Erie, D. A. (2005) DNA mismatch repair, *Annu. Rev. Biochem. 74*, 681−710.
21. Chalikian, T. V., Volker, J., Plum, G. E., and Breslauer, K. J. (1999) A more unified picture for the thermodynamics of nucleic acid duplex melting: A characterization by calorimetric and volumetric techniques, *Proc. Natl. Acad. Sci. U.S.A. 96*, 7853−7858.
22. Tikhomirova, A., Taulier, N., and Chalikian, T. V. (2004) Energetics of nucleic acid stability: The effect of ΔC_P, *J. Am. Chem. Soc. 126*, 16387−16394.
23. Holbrook, J. A., Capp, M. W., Saecker, R. M., and Record, M. T., Jr. (1999) Enthalpy and heat capacity changes for formation of an oligomeric DNA duplex: Interpretation in terms of coupled processes of formation and association of single-stranded helices, *Biochemistry 38*, 8409−8422.
24. Jelesarov, I., Crane-Robinson, C., and Privalov, P. L. (1999) The energetics of HMG box interactions with DNA: Thermodynamic description of the target DNA duplexes, *J. Mol. Biol. 294*, 981−995.
25. Rouzina, I., and Bloomfield, V. A. (1999) Heat capacity effects on the melting of DNA. 2. Analysis of nearest-neighbor base pair effects, *Biophys. J. 77*, 3252−3255.
26. Rouzina, I., and Bloomfield, V. A. (1999) Heat capacity effects on the melting of DNA. 1. General aspects, *Biophys. J. 77*, 3242−3251.
27. Mikulecky, P. J., and Feig, A. L. (2002) Cold denaturation of the hammerhead ribozyme, *J. Am. Chem. Soc. 124*, 890−891.
28. Mikulecky, P. J., and Feig, A. L. (2004) Heat capacity changes in RNA folding: Application of perturbation theory to hammerhead ribozyme cold denaturation, *Nucleic Acids Res. 32*, 3967−3976.
29. Takach, J. C., Mikulecky, P. J., and Feig, A. L. (2004) Salt-dependent heat capacity changes for RNA duplex formation, *J. Am. Chem. Soc. 126*, 6530−6531.
30. Mikulecky, P. J., and Feig, A. L. (2006) Heat capacity changes associated with nucleic acid folding, *Biopolymers 82*, 38−58.
31. Privalov, P. L., and Potekhin, S. A. (1986) Scanning microcalorimetry in studying temperature-induced changes in proteins, *Methods Enzymol. 131*, 4−51.
32. Privalov, G. P., and Privalov, P. L. (2000) Problems and prospects in microcalorimetry of biological macromolecules, *Methods Enzymol. 323*, 31−62.
33. Breslauer, K. J., Freire, E., and Straume, M. (1992) Calorimetry: A tool for DNA and ligand-DNA studies, *Methods Enzymol. 211*, 533−567.
34. Peyret, N., Seneviratne, P. A., Allawi, H. T., and SantaLucia, J., Jr. (1999) Nearest-neighbor thermodynamics and NMR of DNA sequences with internal AA, CC, GG, and TT mismatches, *Biochemistry 38*, 3468−3477.
35. SantaLucia, J., Jr., and Hicks, D. (2004) The thermodynamics of DNA structural motifs, *Annu. Rev. Biophys. Biomol. Struct. 33*, 415−440.
36. Sugimoto, N., Nakano, M., and Nakano, S. (2000) Thermodynamics-structure relationship of single mismatches in RNA/DNA duplexes, *Biochemistry 39*, 11270−11281.
37. Marky, L. A., and Breslauer, K. J. (1987) Calculating thermodynamic data for transitions of any molecularity from equilibrium melting curves, *Biopolymers 26*, 1601−1620.
38. Gelfand, C. A., Plum, G. E., Grollman, A. P., Johnson, F., and Breslauer, K. J. (1998) Thermodynamic consequences of an abasic lesion in duplex DNA are strongly dependent on base sequence, *Biochemistry 37*, 7321−7327.
39. Cantor, C. R., Warshaw, M. M., and Shapiro, H. (1970) Oligonucleotide Interactions. 3. Circular Dichroism Studies of Conformation of Deoxyoligonucleotides, *Biopolymers 9*, 1059−1077.
40. Kallansrud, G., and Ward, B. (1996) A comparison of measured and calculated single- and double-stranded oligodeoxynucleotide extinction coefficients, *Anal. Biochem. 236*, 134−138.
41. Murphy, J. H., and Trapane, T. L. (1996) Concentration and extinction coefficient determination for oligonucleotides and analogs using a general phosphate analysis, *Anal. Biochem. 240*, 273−282.
42. Henderson, J. T., Benight, A. S., and Hanlon, S. (1992) A Semi-Micromethod for the Determination of the Extinction Coefficients of Duplex and Single-Stranded DNA, *Anal. Biochem. 201*, 17−29.
43. Cavaluzzi, M. J., and Borer, P. N. (2004) Revised UV extinction coefficients for nucleoside-5′-monophosphates and unpaired DNA and RNA, *Nucleic Acids Res. 32*, e13.

44. Breslauer, K. J. (1995) Extracting thermodynamic data from equilibrium melting curves for oligonucleotide order−disorder transitions, *Methods Enzymol. 259*, 221−242.
45. Gray, D. M., Ratliff, R. L., and Vaughan, M. R. (1992) Circular dichroism spectroscopy of DNA, *Methods Enzymol. 211*, 389−406.
46. Gray, D. M., Hung, S. H., and Johnson, K. H. (1995) Absorption and circular dichroism spectroscopy of nucleic acid duplexes and triplexes, *Methods Enzymol. 246*, 19−34.
47. Owczarzy, R., You, Y., Moreira, B. G., Manthey, J. A., Huang, L., Behlke, M. A., and Walder, J. A. (2004) Effects of sodium ions on DNA duplex oligomers: Improved predictions of melting temperatures, *Biochemistry 43*, 3537−3554.
48. Ke, S. H., and Wartell, R. M. (1993) Influence of nearest neighbor sequence on the stability of base pair mismatches in long DNA: Determination by temperature-gradient gel electrophoresis, *Nucleic Acids Res. 21*, 5137−5143.
49. Kaya, H., and Chan, H. S. (2000) Polymer principles of protein calorimetric two-state cooperativity, *Proteins 40*, 637−661.
50. Breslauer, K. J., Frank, R., Blocker, H., and Marky, L. A. (1986) Predicting DNA duplex stability from the base sequence, *Proc. Natl. Acad. Sci. U.S.A. 83*, 3746−3750.
51. Gelfand, C. A., Plum, G. E., Grollman, A. P., Johnson, F., and Breslauer, K. J. (1998) The impact of an exocyclic cytosine adduct on DNA duplex properties: Significant thermodynamic consequences despite modest lesion-induced structural alterations, *Biochemistry 37*, 12507−12512.

BI060304J